Macular Choroidal Thickness and Volume in Healthy Pediatric Individuals Measured by Swept-Source Optical Coherence Tomography

Toshihiko Nagasawa,[1,2] Yoshinori Mitamura,[3] Takashi Katome,[3] Kayo Shinomiya,[3] Takeshi Naito,[3] Daisuke Nagasato,[1] Yukiko Shimizu,[1] Hitoshi Tabuchi,[1] and Yoshiaki Kiuchi[2]

[1]Department of Ophthalmology, Saneikai Tsukazaki Hospital, Himeji, Japan
[2]Department of Ophthalmology and Visual Sciences, Graduate School of Biomedical Sciences, Hiroshima University, Hiroshima, Japan
[3]Department of Ophthalmology, Institute of Health Biosciences, The University of Tokushima Graduate School, Tokushima, Japan

Correspondence: Yoshinori Mitamura, Department of Ophthalmology, Institute of Health Biosciences, The University of Tokushima Graduate School, 3-18-15 Kuramoto, Tokushima 770-8503, Japan; ymita@tokushima-u.ac.jp.

Submitted: May 3, 2013
Accepted: September 22, 2013

Citation: Nagasawa T, Mitamura Y, Katome T, et al. Macular choroidal thickness and volume in healthy pediatric individuals measured by swept-source optical coherence tomography. *Invest Ophthalmol Vis Sci*. 2013;54:7068–7074. DOI:10.1167/iovs.13-12350

Purpose. We evaluated the choroidal thickness and volume in healthy pediatric individuals by swept-source optical coherence tomography (SS-OCT) and compared the findings to those of adults.

Methods. We examined 100 eyes of 100 healthy pediatric volunteers (3–15 years) and 83 eyes of 83 healthy adult volunteers (24–87 years) by SS-OCT with a tunable long wavelength laser source. The three-dimensional raster scan protocol was used to construct a choroidal thickness map. When the built-in software delineated an erroneous chorioscleral border in the B-scan images, manual segmentation was used.

Results. The central choroidal thickness and volume within a 1.0-mm circle were significantly larger in the children (260.4 ± 57.2 μm, 0.205 ± 0.045 mm^3) than in the adults (206.1 ± 72.5 μm, 0.160 ± 0.056 mm^3, both $P < 0.0001$). In the children, the mean choroidal thickness of the nasal area was significantly thinner than that of all other areas ($P < 0.005$). Pediatric choroidal thinning with increasing age in the central area was faster than that in the outer areas. Stepwise regression analysis showed that the axial length and body mass index had the highest correlation with the choroidal thickness ($R^2 = 0.313$, $P < 0.0001$).

Conclusions. The macular choroidal thickness and volume in the pediatric individuals were significantly larger than those in the adults. The pediatric choroidal thinning with increasing age is more rapid in the central area. Pediatric choroidal thickness is associated with several systemic or ocular parameters, especially the axial length and body mass index. These differences should be remembered when the choroidal thickness is evaluated in pediatric patients with retinochoroidal diseases.

Keywords: swept-source optical coherence tomography, choroidal thickness, choroidal volume, pediatric individual, adult

Enhanced depth imaging (EDI) optical coherence tomography (OCT) based on spectral-domain OCT (SD-OCT) technology has allowed clinicians to examine the choroidal thickness in healthy eyes and eyes with various pathologies.[1–6]

Swept-source OCT (SS-OCT) uses a swept wavelength laser as the light source,[7,8] and a recently developed SS-OCT instrument has an A-scan repetition rate of 100,000 Hz. When the coherence length of the source is appropriate, SS-OCT can achieve much less roll-off in sensitivity with increasing depth than with the standard SD-OCT.[9] In addition, the current SS-OCT instrument uses a longer center wavelength, which improved its ability to penetrate deeply into tissues.

With this SS-OCT instrument, precise evaluations of deeper structures of the eye, such as the choroid and retrobulbar optic nerve, are possible.[10] Ikuno et al.[11] studied the choroidal thickness of healthy adult subjects with an SS-OCT. Because the current SS-OCT instrument has a high scan rate and a relatively low sensitivity roll-off versus depth, a three-dimensional (3D) high contrast image of the choroid can be obtained.[12–14] Recently, Hirata et al.[15] constructed a choroidal thickness map using the 3D raster scan protocol of the SS-OCT, and they investigated the macular choroidal thickness and volume of healthy adults.

The choroidal thickness determined by EDI-OCT or SS-OCT has been reported to decrease with age in healthy adult eyes.[3,11,15–18] However, information on the choroidal thickness in children remains limited.[19–21] In these studies, the choroidal thickness of only a few sampling points[19,20] or the average choroidal thickness on the scan line[21] was examined. Thus, the exact choroidal thickness could not be determined, because the thickness can be affected by focal changes,[22,23] and by irregularities of the chorioscleral border.[5] In addition, the location of the chorioscleral border was done manually. It would be better to construct a map of the choroid with the borders selected objectively to overcome these limitations.

Thus, the purpose of this study was to determine the choroidal thickness and volume by constructing choroidal thickness maps in a pediatric population. To accomplish this,

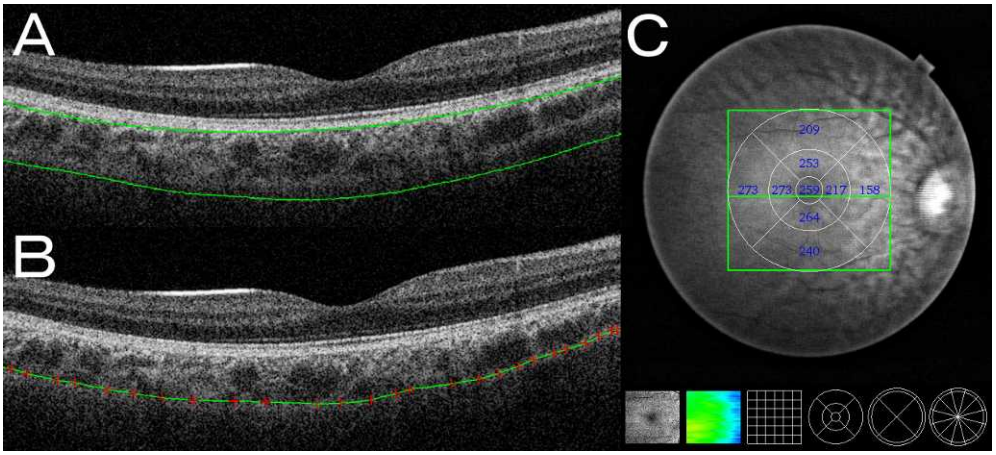

FIGURE 1. Choroidal thickness map of a healthy 7-year-old boy obtained by SS-OCT. The 3D raster scan protocol with 512 A-scans × 256 B-scans was used to obtain 3D imaging data of the 6 × 6-mm area. (**A**) Erroneous placement of the chorioscleral border made by the automatic built-in software in one of the B-scan images of the 3D data set. Although the tracing of the retinal pigment epithelium is correct, that of the chorioscleral border is not accurate. (**B**) Manual segmentation of the chorioscleral border in the same B-scan image. Only when the built-in software delineated an erroneous chorioscleral border, manual segmentation was performed. (**C**) By analyzing the B-scan images of the 3D data set, a choroidal thickness map of the 6 × 6-mm area centered on the fovea was created. By applying the ETDRS grid to the map, the mean choroidal thickness was obtained for each sector.

we scanned the macular area of healthy pediatric eyes using the 3D raster scan protocol, and constructed a choroidal thickness map. By using the Early Treatment Diabetic Retinopathy Study (ETDRS)[24] grid for the choroidal thickness maps, we were able to determine the mean choroidal thickness and volume in each sector of the grid. The findings obtained from the pediatric individuals were compared to those obtained from adults.

SUBJECTS AND METHODS

We studied 100 eyes of 100 healthy pediatric volunteers, with a mean ± SD age of 7.9 ± 3.1 years and a range from 3 to 15 years (45 boys and 55 girls), and 83 eyes of 83 healthy adult volunteers, with a mean age of 54.5 ± 19.3 years and a range from 24 to 87 years (43 men and 40 women) at Saneikai Tsukazaki Hospital and Tokushima University Hospital. All subjects had no ophthalmic or systemic signs or symptoms. One eye was chosen randomly for the statistical analyses. The procedures used conformed to the tenets of the Declaration of Helsinki, and an informed consent was obtained from either the subjects or their legal guardians after explanation of the nature and possible consequences of the study. An approval was obtained from the Institutional Review Board of Saneikai Tsukazaki Hospital and Tokushima University Hospital to perform this study.

All subjects underwent standard ophthalmologic examinations, including measurements of the best-corrected visual acuity (BCVA), applanation tonometry, slit-lamp biomicroscopy, indirect ophthalmoscopy, autorefractometry (ARK1; Nidek, Gamagori, Japan), and axial length measurements with the IOLMaster (Carl Zeiss Meditec, Jena, Germany). All of the examinations were performed on the same day. The BCVA was measured with a standard Japanese Landolt visual acuity chart. All of the healthy pediatric volunteers had a BCVA that ranged from 0.6 to 1.5, and all adults had a BCVA that ranged from 0.9 to 1.5. The body height and weight were recorded, and the body mass index was calculated for each subject. The exclusion criteria included history of intraocular surgery; history or evidence of chorioretinal or vitreoretinal diseases, such as central serous chorioretinopathy; refractive errors (spherical equivalent) greater than ±6 diopters (D); and evidence of glaucoma. Subjects with systemic disease that might affect the choroidal thickness, such as diabetes mellitus, also were excluded.

Swept-source Optical Coherence Tomography

The macular area of the eyes was examined with the SS-OCT instrument (DRI OCT-1; Topcon, Tokyo, Japan), which was government approved for use in Japan. The light source of this SS-OCT system is a wavelength tunable laser centered at 1050 nm with an approximate 100-nm tuning range. The tissue imaging depth was 2.6 mm.

After pupillary dilation, the SS-OCT examinations were performed by trained examiners. The 3D volumetric raster scan protocol was used, and 3D volumetric data were acquired in 0.8 seconds. Each 3D scan covered an area of 6 × 6 mm centered on the fovea with 512 A-scans × 256 B-scans. To improve the image quality, 4 consecutive B-scan images of the same area were averaged. Because of the infrared scanning light, eye movements during the scans were minimized. All examinations were performed from 2:00 PM to 5:00 PM to reduce the effects of diurnal variations.[25,26]

Choroidal Thickness and Volume Measurement

From a series of 64 B-scan OCT images, each of which was created by averaging 4 consecutive B-scans, a choroidal thickness map of a 6 × 6 mm area was created by semiautomatic segmentation. Using the built-in software, the choroidal thickness was measured as the distance between the outer border of the RPE and the inner surface of the chorioscleral border. In the analyses of the 64 B-scan images, each scanned OCT image was examined to be certain that a proper tracing of the chorioscleral border had been made. When the built-in software delineated an inaccurate chorioscleral border (Fig. 1A), a manual segmentation was made by trained observers in a masked fashion (Fig. 1B).

The ETDRS grid was used for the choroidal thickness map (Fig. 1C), and the mean regional thicknesses were calculated for the nine sectors of the grid.[15,27] The inner and outer rings had diameters of 1 to 3 and 3 to 6 mm, respectively, and they were divided into superior, inferior, temporal, and nasal

Table 1. Comparisons of the Choroidal Thickness and Volume Between Healthy Pediatric and Adult Individuals

	Pediatric Individuals	Adult Individuals	*P* Value
Eyes, *n*	100	83	
Mean age, y	7.9 ± 3.1	54.5 ± 19.3	<0.0001
Mean axial length, mm	23.13 ± 1.37	24.14 ± 1.17	<0.0001
Mean refractive error, D	−0.04 ± 1.96	−0.25 ± 2.42	0.5256
Central choroidal thickness, 1.0-mm circle, μm	260.4 ± 57.2	206.1 ± 72.5	<0.0001
Macular choroidal thickness, 3.0-mm circle, μm	255.2 ± 52.3	201.8 ± 68.6	<0.0001
Macular choroidal thickness, 6.0-mm circle, μm	240.3 ± 45.6	190.8 ± 63.2	<0.0001
Central choroidal volume, 1.0-mm circle, mm^3	0.205 ± 0.045	0.160 ± 0.056	<0.0001

quadrants. The individual sectors are referred to as the central, inner temporal, inner superior, inner inferior, inner nasal, outer temporal, outer superior, outer inferior, and outer nasal sectors. In addition, the macular choroidal thickness within a circle of 3.0- or 6.0-mm diameter, and within an inner or outer ring was calculated. Based on the choroidal thicknesses obtained, we calculated the choroidal volume for each sector of the ETDRS grid.

Measurement of Reproducibility

Because the segmentation was done manually in some images, we evaluated the interobserver reproducibility of the corrections. The chorioscleral border in the OCT images of one raster scan was adjusted by two observers in 14 selected pediatric individuals before the study.[15] The thickness maps and mean choroidal thicknesses were calculated independently, and the intraclass correlation coefficient (ICC) for each ETDRS sector was calculated.

In addition, the methods described by Bland and Altman[28] was used to evaluate interobserver reproducibility.[29] The mean difference between two choroidal thickness measurements (Observer 1 − Observer 2) for each of the 14 individuals represented the bias. The 95% limits of agreement (LoA), the expected difference between two measurements, were calculated as the mean of the differences ± 1.96 × SD of the differences.

Statistical Analyses

Student's *t*-tests were used to determine the significance of the differences in the age, axial length, refractive errors, central or macular choroidal thickness, and central choroidal volume between the pediatric and adult individuals. Data were analyzed using one factor ANOVA and Fisher's post hoc least significant difference (PSLD) test to compare the choroidal thickness or volume in three or more groups. The correlations between choroidal thickness and systemic or ocular parameters were determined by Pearson's correlation tests for simple regression analysis and forward stepwise multiple regression analysis. The differences in the choroidal thickness between boys and girls were tested by χ^2 tests. All analyses were done with the SPSS version 20.0 (SPSS Japan, Tokyo, Japan). A P value < 0.05 was considered statistically significant.

Results

None of the eyes was excluded because of unreliable measurements of the choroidal thickness. Even in pediatric individuals, none of the eyes was excluded because of eye movements during the scanning procedure.

Comparisons of Choroidal Thickness and Volume Between Pediatric and Adult Individuals

The mean axial length in the pediatric individuals was significantly shorter than that in the adults ($P < 0.0001$, Table 1). The mean refractive error in the pediatric individuals was not significantly different from that of the adults ($P = 0.5256$).

The central choroidal thickness and volume within a 1.0-mm circle were significantly greater in the pediatric individuals (260.4 ± 57.2 μm, 0.205 ± 0.045 mm^3, respectively) than in the adults (206.1 ± 72.5 μm, 0.160 ± 0.056 mm^3, respectively; both $P < 0.0001$; Table 1). The macular choroidal thickness within a circle of 3.0- and 6.0-mm diameter in the children was significantly thicker than that of the adults (both $P < 0.0001$).

Choroidal Thickness and Volume in ETDRS Sectors

In the pediatric individuals, the choroidal thicknesses in the four inner and four outer sectors were significantly different (both $P < 0.0001$, Table 2). The inner and outer nasal choroid

Table 2. Choroidal Thickness and Volume in ETDRS Grid Sectors in Pediatric and Adult Individuals

	Pediatric Individuals		Adult Individuals
Area	Choroidal Volume, mm^3	Mean Choroidal Thickness, μm	Mean Choroidal Thickness, μm
Center	0.205 ± 0.045	260.4 ± 57.2	206.1 ± 72.5
Inner temporal	0.423 ± 0.081*	269.4 ± 51.9*	206.3 ± 74.2
Inner superior	0.407 ± 0.086*	259.1 ± 54.4*	212.0 ± 70.6
Inner inferior	0.404 ± 0.084*	257.1 ± 53.8*	202.0 ± 74.7
Inner nasal	0.365 ± 0.091	232.2 ± 58.0	189.6 ± 70.5
Outer temporal	1.388 ± 0.238†	262.0 ± 44.9†	197.7 ± 69.2†
Outer superior	1.327 ± 0.249†	250.3 ± 47.0†	213.4 ± 69.7†
Outer inferior	1.300 ± 0.255†	245.2 ± 48.1†	194.6 ± 68.9†
Outer nasal	0.971 ± 0.296	182.7 ± 53.0	147.8 ± 60.9

* Significantly larger than values of inner nasal area ($P < 0.005$).
† Significantly larger than values of outer nasal area ($P < 0.0001$).

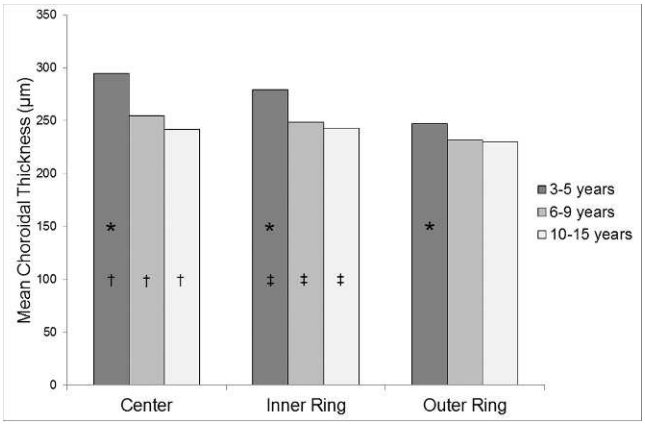

Figure 2. Pediatric choroidal thinning with increasing age in the central, inner ring, and outer ring areas of ETDRS grid. The mean choroidal thicknesses in the 3- to 5-year-old ($n = 25$), 6- to 9-year-old ($n = 42$), and 10- to 15-year-old ($n = 33$) age groups are presented. The choroidal thinning with increasing age appears to be more rapid in the central area than in the inner and outer rings. *$P = 0.0057$, †$P = 0.0011$, ‡$P = 0.0191$.

was significantly thinner than choroid of the other three inner and outer sectors (all $P < 0.005$). The choroidal thickness of the temporal sector was the thickest followed by the superior, inferior, and nasal choroid. However, differences among the temporal, superior, and inferior sectors of the inner and outer rings were not statistically significant.

In the adults, the choroidal thicknesses of the four inner sectors were not significantly different ($P = 0.2347$), but the outer choroidal thicknesses were significantly different among the four sectors ($P < 0.0001$). The outer nasal choroid was significantly thinner than that of the other three outer sectors (all $P < 0.0001$). The superior choroid was thickest, followed by the temporal, inferior, and nasal choroid; however, the majority of the differences were not significant.

Changes of the choroidal thickness maps associated with age are presented in Figure 2 and Table 3. In the pediatric individuals, the choroidal thinning with increasing age appeared to be more rapid in the central area than in the inner and outer rings (Fig. 2). The differences in the mean choroidal thicknesses among the 3- to 5-year-old, 6- to 9-year-old, and 10- to 15-year-old age groups were significant in the central and inner ring areas ($P = 0.0011$, $P = 0.0191$, respectively), but not in the outer ring area ($P = 0.2551$). The differences in the mean choroidal thicknesses of the central, inner ring, and outer ring areas were significant in the 3- to 5-year-old age group ($P = 0.0057$), but not in the 6- to 9-year-old and 10- to 15-year-old age groups ($P = 0.1081$, $P = 0.4401$, respectively), with a rapid decrease in the central

Table 3. Changes of the Mean Choroidal Thickness in ETDRS Grid Associated With Age

	Eyes, *n*	Center, μm	Inner Ring, μm	Outer Ring, μm
Pediatric individuals				
3–15 y	100	260.4 ± 57.2	254.4 ± 52.0	235.0 ± 43.3
Adult individuals				
24–40 y	25	247.7 ± 51.6	241.7 ± 49.8	229.1 ± 44.4
41–55 y	14	221.5 ± 67.2	220.1 ± 63.4	203.4 ± 45.4
56–70 y	19	190.1 ± 71.3	189.2 ± 68.1	172.8 ± 62.9
71–87 y	25	168.1 ± 73.3	163.5 ± 69.4	151.1 ± 57.9

Table 4. Simple Regression Analysis for Correlations Between the Mean Choroidal Thickness of the Macular Area and the Age, Axial Length, Body Height, Body Weight, Body Mass Index, or Refractive Error in Pediatric Individuals

	Central Choroidal Thickness, 1.0-mm Circle, μm	Macular Choroidal Thickness, 6.0-mm Circle, μm
Age, y	$r = -0.404$	$r = -0.274$
	$P < 0.0001$	$P = 0.0056$
Axial length, mm	$r = -0.525$	$r = -0.448$
	$P < 0.0001$	$P < 0.0001$
Body height, cm	$r = -0.419$	$r = -0.299$
	$P < 0.0001$	$P = 0.0024$
Body weight, kg	$r = -0.412$	$r = -0.329$
	$P < 0.0001$	$P = 0.0008$
Body mass index	$r = -0.293$	$r = -0.272$
	$P = 0.0030$	$P = 0.0060$
Refractive error, D	$r = 0.325$	$r = 0.297$
	$P = 0.0009$	$P = 0.0025$

choroidal thickness. In pediatric and adult individuals. The most remarkable decrease in choroidal thickness was seen between the 41- to 55-year-old and 56- to 70-year-old groups, although some of the adult age groups had only a small number of eyes (Table 3).

Simple Regression Analysis for Correlations Between Choroidal Thickness, and Systemic and Ocular Parameters in Pediatric Individuals

Simple linear regression analysis showed that the central choroidal thickness was correlated significantly with the age, axial length, body height, body weight, body mass index, and refractive error (all $P < 0.005$, Table 4). The central choroidal thickness was significantly thicker in girls (274.1 ± 62.1 μm) than in boys (247.9 ± 46.6 μm, $P = 0.0255$). The correlations between the macular choroidal thickness within a circle of 6.0-mm diameter and systemic and ocular parameters were similar to the results for the central choroidal thickness (Table 4).

Multiple Regression Analysis for Correlations Between Choroidal Thickness, and Systemic and Ocular Parameters in Pediatric Individuals

Multiple linear regression analysis of the mean central choroidal thickness by age, axial length, body height, body weight, body mass index, and refractive error was performed. A forward stepwise method was used to determine factors associated most with the choroidal thickness. The highest correlation was between the choroidal thickness, and the axial length and body mass index, with a determination coefficient (R^2) of 0.313 ($P < 0.0001$, Fig. 3). Using analysis of covariance, the effects of the age group (pediatric or adult group), axial length, and body mass index on the central choroidal thickness were evaluated. After adjustment for the axial length and body mass index, the central choroidal thickness was no longer significantly correlated with the age group ($P = 0.632$).

Interobserver Reproducibility of Choroidal Thickness

In all the pediatric and adult individuals, manual segmentation was performed in 180 of the 183 eyes. Proportion of the scans needed for manual segmentation to all the 64 scans was calculated in each subject. The mean percentage of manual

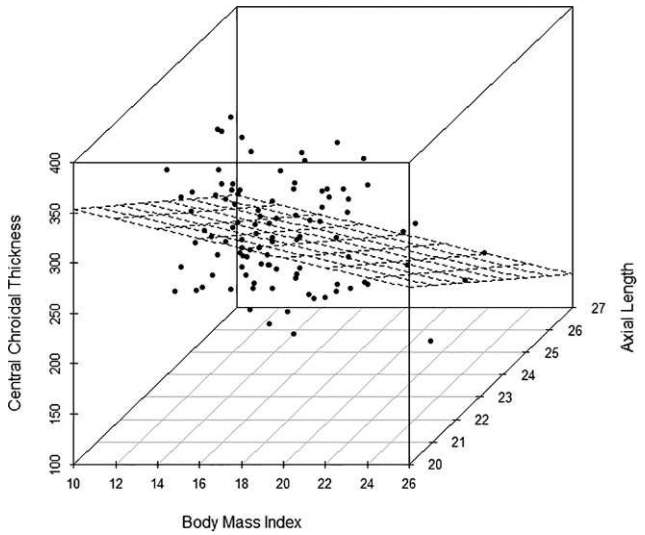

FIGURE 3. Three-dimensional scatterplot of the body mass index (*x*-axis), central choroidal thickness (*y*-axis), and axial length (*z*-axis). The model shows a relatively good coefficient of determination ($R^2 = 0.313$, $P < 0.0001$). Mean central choroidal thickness = 807.933 − 20.229 × axial length − 4.906 × body mass index.

segmentation required was 25.1 ± 20.7%. A proper tracing of the RPE was confirmed in all images of all subjects.

Before this study, the choriosclera border was corrected independently by the two observers in 14 pediatric individuals.[15] The ICCs for the mean choroidal thickness of each ETDRS grid sector that was measured by the two observers are shown in Table 5. The mean choroidal thickness had a high ICC (from 0.9908–0.9995) between the two observers ($P < 0.0001$).

For the Bland and Altman plots, the mean difference in the choroidal thickness of the nine ETDRS grid sectors between Observer 1 and Observer 2 varied from −1.9 to 2.9 μm. The 95% LoA for all the ETDRS sectors including zero showed that no fixed bias was present (Table 5). In all of the ETDRS sectors, the mean of choroidal thickness calculated by Observer 1 and Observer 2 was not correlated significantly with the mean difference between the two measurements (Observer 1 − Observer 2, all $P > 0.05$). Thus, no proportional bias was considered to be present.

TABLE 5. ICCs and Results of Bland-Altman Method in Choroidal Thickness of ETDRS Grid Sectors Measured by Two Observers in 14 Selected Pediatric Individuals

Area	ICC (*P* Value)	95% LoA	Correlation Between Mean and Mean Difference
Center	0.9979 (<0.0001)	−13.5∼11.5	$r = -0.260$
			$P = 0.3783$
Inner temporal	0.9995 (<0.0001)	−5.4∼4.8	$r = -0.271$
			$P = 0.3563$
Inner superior	0.9908 (<0.0001)	−20.8∼17.1	$r = -0.207$
			$P = 0.4869$
Inner inferior	0.9992 (<0.0001)	−7.2∼6.9	$r = -0.147$
			$P = 0.6224$
Inner nasal	0.9962 (<0.0001)	−16.1∼12.9	$r = -0.308$
			$P = 0.2908$
Outer temporal	0.9945 (<0.0001)	−9.6∼14.6	$r = -0.234$
			$P = 0.4284$
Outer superior	0.9931 (<0.0001)	−12.6∼18.4	$r = 0.356$
			$P = 0.2169$
Outer inferior	0.9993 (<0.0001)	−7.0∼5.6	$r = -0.513$
			$P = 0.0602$
Outer nasal	0.9953 (<0.0001)	−13.9∼17.2	$r = 0.151$
			$P = 0.6129$

The 95% LoA, expected difference between two measurements was calculated as the mean of the differences ± 1.96 × SD of the differences.

DISCUSSION

Our findings showed that high ICC values were found between the two observers, and the results of Bland-Altman plots indicated the highly reproducible measurements of the choroidal thickness with semiautomatic segmentation. These findings indicated that we can obtain valid and reproducible results of the choroidal thickness of the images obtained by SS-OCT.

Park and Oh[20] reported that the pediatric subfoveal choroidal thickness determined by EDI-OCT was 343.1 ± 79.8 μm. However, the choroidal thickness was measured in a point-by-point way and did not include comparisons with adult subjects. Ruiz-Moreno et al.[19] examined the choroidal thickness in 43 normal pediatric patients using a prototype SS-OCT instrument. They reported that the mean macular choroidal thickness in the pediatric patients (285.2 ± 56.7 μm) was not significantly thicker than that in healthy adults (275.2 ± 92.7 μm, $P = 0.08$). However, they measured the choroidal thickness at only 7 points in the horizontal plane. In addition, the mean age of their pediatric subjects was 10 ± 3 years, which is older than that of our group. Moreover, both eyes were included in their analyses, which can lead to bias. We examined the mean choroidal thickness and volume in one randomly selected eye of all subjects to create the choroidal thickness maps.

Using EDI-OCT, Read et al.[21] recently reported that the choroidal thickness increased significantly from early childhood to adolescence. However, only children with refractive error between +1.25 and −0.50 D were studied, thereby minimizing the potential influence of refractive error or axial length on the choroidal thickness. Indeed, the investigators reported that a strong negative association between axial length and choroidal thickness would be expected to result in a decrease in choroidal thickness with increasing age, rather than an increase in choroidal thickness. They concluded that longitudinal studies of the choroidal thickness in childhood, including myopic participants, will be necessary.

An earlier study reported that the axial length increased by 3 mm between the ages of 9 months and 9 years.[30] Because the choroidal thickness decreases with increases in the axial length in healthy adults,[11,15,16] the choroidal thickness in children is assumed to be thicker than that of adults. We found that the macular choroid was significantly thicker and the volume significantly larger in the pediatric individuals than in the adults. After adjustment for axial length and body mass index, the central choroidal thickness was no longer significantly correlated with the age group. This suggests that the pediatric choroidal thickening may be influenced by the shortening of the axial length and low body mass index. Hirata et al.[15] reported that the central choroidal thickness was 202.6 ± 83.5 μm in adults, which is comparable to the 206.1 ± 72.5 in our study.

The sectorial choroidal thicknesses were slightly different in the pediatric and adult individuals. Although the thinnest area was nasal in both groups, the thickest area was temporal in the

children and superior in the adults. Ruiz-Moreno et al.[19] reported that the pediatric choroidal thickness along the horizontal line was thicker on the temporal side than in the fovea, and it was thinnest on the nasal side. In addition, the adult choroidal thickness in their study was thickest in the fovea, followed by the temporal, and it was thinnest on the nasal side. These results are consistent with our results.

The thinning of pediatric choroid with increasing age appeared to occur more quickly in the central area. Moreno et al.[31] reported that the central choroidal thickness in newborn infants (329 ± 66 μm) was remarkably thicker than that in adults (258 ± 66 μm). In their study, the subfoveal choroid in the newborn infant was significantly thicker than the superior or inferior choroid at 2000 μm from the fovea, and the mean difference between subfoveal and superior choroidal thickness was 87 μm. These results are consistent with our findings.

To the best of our knowledge, there has been only one report on the choroidal volume measured by SS-OCT in adults.[15] The choroidal volume can reflect the vascular changes, for example, vascular hyperpermeability or vasodilation, that can be observed in retinochoroidal diseases, such as central serous chorioretinopathy.[4] At present, the status of the choroid usually is evaluated by the choroidal thickness measured at a few points. However, point-by-point measurements can be affected by focal thickening or thinning of the choroid,[22,23] or by irregularities of the choroscleral border.[5] Examining the choroidal volume by 3D mapping is a better method for a comprehensive evaluation of the entire macular area.

In pediatric individuals, Ruiz-Moreno et al.[19] reported that the average choroidal thickness at 7 horizontal points of the macular area was correlated significantly with the age and refractive error. We found that the mean central choroidal thickness was correlated significantly with the age, axial length, body height, body weight, body mass index, and refractive error using simple linear regression analyses. In addition, multiple linear regression analysis with the forward stepwise method showed that the model determined by the axial length and body mass index had the highest regression coefficients. In schoolchildren, Selovic et al.[32] found that the axial length increased with increasing age, body height, and weight, but was more highly correlated with the height and weight than with the age. This close relationship between axial length and body height or weight may contribute to the relationship between pediatric choroidal thickness and body mass index, because the axial length is known to be correlated closely with the choroidal thickness.[11,15,16]

A choroidal thickness map of the macular area was created by semiautomatic segmentation. Manual segmentation was performed in 25.1 ± 20.7% of our eyes because of errors in the delineation of the choroscleral border by the built-in software. To standardize this evaluation further, it will be necessary that a choroidal thickness map can be created by fully automatic segmentation. For this purpose, a software to determine choroscleral border more accurately and further improvement of the OCT image quality are essential.

One of the limitations of our study was that we examined only Japanese subjects, and the choroidal thickness in children of other races was not determined. In addition, the relatively small sample size might be insufficient to evaluate choroidal thicknesses in a pediatric population.

In conclusion, the macular choroid was significantly thicker and the volume was significantly larger in pediatric individuals than in adults. Although the thinnest area was nasal in both groups, the thickest area was temporal in the children and superior in the adults. Pediatric choroidal thinning with increasing age appears to be more rapid in the central sector than in the outer sectors. Pediatric choroidal thickness was associated significantly with systemic and ocular parameters, especially the axial length and body mass index. Further studies in a larger number of pediatric individuals will be needed to determine precisely the choroidal status in pediatric eyes.

Acknowledgments

The authors alone are responsible for the content and writing of the paper.

Disclosure: **T. Nagasawa**, None; **Y. Mitamura**, None; **T. Katome**, None; **K. Shinomiya**, None; T**. Naito**, None; **D. Nagasato**, None; **Y. Shimizu**, None; **H. Tabuchi**, None; **Y. Kiuchi**, None

References

1. Spaide RF, Koizumi H, Pozzoni MC. Enhanced depth imaging spectral-domain optical coherence tomography. *Am J Ophthalmol*. 2008;146:496–500.
2. Spaide RF. Enhanced depth imaging optical coherence tomography of retinal pigment epithelial detachment in age-related macular degeneration. *Am J Ophthalmol*. 2009;147:644–652.
3. Margolis R, Spaide RF. A pilot study of enhanced depth imaging optical coherence tomography of the choroid in normal eyes. *Am J Ophthalmol*. 2009;147:811–815.
4. Imamura Y, Fujiwara T, Margolis R, Spaide RF. Enhanced depth imaging optical coherence tomography of the choroid in central serous chorioretinopathy. *Retina*. 2009;29:1469–1473.
5. Chung SE, Kang SW, Lee JH, Kim YT. Choroidal thickness in polypoidal choroidal vasculopathy and exudative age-related macular degeneration. *Ophthalmology*. 2011;118:840–845.
6. Fong AH, Li KK, Wong D. Choroidal evaluation using enhanced depth imaging spectral-domain optical coherence tomography in Vogt-Koyanagi-Harada disease. *Retina*. 2011;31:502–509.
7. Ohno-Matsui K, Akiba M, Moriyama M, Ishibashi T, Tokoro T, Spaide RF. Imaging retrobulbar subarachnoid space around optic nerve by swept-source optical coherence tomography in eyes with pathologic myopia. *Invest Ophthalmol Vis Sci*. 2011;52:9644–9650.
8. Spaide RF, Akiba M, Ohno-Matsui K. Evaluation of peripapillary intrachoroidal cavitation with swept source and enhanced depth imaging optical coherence tomography. *Retina*. 2012;32:1037–1044.
9. Wojtkowski M, Srinivasan V, Ko T, Fujimoto J, Kowalczyk A, Duker J. Ultrahigh-resolution, high-speed, Fourier domain optical coherence tomography and methods for dispersion compensation. *Opt Express*. 2004;12:2404–2422.
10. Nagasawa T, Mitamura Y, Katome T, Nagasato D, Tabuchi H. Swept-source optical coherence tomographic findings in morning glory syndrome [published online ahead of print May 28, 2013]. *Retina*.
11. Ikuno Y, Kawaguchi K, Nouchi T, Yasuno Y. Choroidal thickness in healthy Japanese subjects. *Invest Ophthalmol Vis Sci*. 2010;51:2173–2176.
12. Potsaid B, Baumann B, Huang D, et al. Ultrahigh speed 1050 nm swept source/Fourier domain OCT retinal and anterior segment imaging at 100,000 to 400,000 axial scans per second. *Opt Express*. 2010;18:20029–20048.
13. Srinivasan VJ, Huber R, Gorczynska I, et al. High-speed, high resolution optical coherence tomography retinal imaging with a frequency-swept laser at 850 nm. *Opt Lett*. 2007;32:361–363.
14. Yasuno Y, Hong Y, Makita S, et al. In vivo high-contrast imaging of deep posterior eye by 1-micron swept source optical coherence tomography and scattering optical coherence angiography. *Opt Express*. 2007;15:6121–6139.

15. Hirata M, Tsujikawa A, Matsumoto A, et al. Macular choroidal thickness and volume in normal subjects measured by swept-source optical coherence tomography. *Invest Ophthalmol Vis Sci*. 2011;52:4971–4978.
16. Ding X, Li J, Zeng J, et al. Choroidal thickness in healthy Chinese subjects. *Invest Ophthalmol Vis Sci*. 2011;52:9555–9560.
17. Ouyang Y, Heussen FM, Mokwa N, et al. Spatial distribution of posterior pole choroidal thickness by spectral domain optical coherence tomography. *Invest Ophthalmol Vis Sci*. 2011;52:7019–7026.
18. Manjunath V, Taha M, Fujimoto JG, Duker JS. Choroidal thickness in normal eyes measured using Cirrus HD optical coherence tomography. *Am J Ophthalmol*. 2010;150:325–329.
19. Ruiz-Moreno JM, Flores-Moreno I, Lugo F, Ruiz-Medrano J, Montero JA, Akiba M. Macular choroidal thickness in normal pediatric individuals measured by swept-source optical coherence tomography. *Invest Ophthalmol Vis Sci*. 2013;54:353–359.
20. Park KA, Oh SY. Analysis of spectral-domain optical coherence tomography in preterm children: retinal layer thickness and choroidal thickness profiles. *Invest Ophthalmol Vis Sci*. 2012;53:7201–7207.
21. Read SA, Collins MJ, Vincent SJ, Alonso-Caneiro D. Choroidal thickness in childhood. *Invest Ophthalmol Vis Sci*. 2013;54:3586–3593.
22. Yeoh J, Rahman W, Chen F, et al. Choroidal imaging in inherited retinal disease using the technique of enhanced depth imaging optical coherence tomography. *Graefes Arch Clin Exp Ophthalmol*. 2010;248:1719–1728.
23. Yasuno Y, Okamoto F, Kawana K, Yatagai T, Oshika T. Investigation of multifocal choroiditis with panuveitis by three-dimensional high-penetration optical coherence tomography. *J Biophotonics*. 2009;2:435–441.
24. Early Treatment Diabetic Retinopathy Study research group. Photocoagulation for diabetic macular edema. Early Treatment Diabetic Retinopathy Study report number 1. *Arch Ophthalmol*. 1985;103:1796–1806.
25. Brown JS, Flitcroft DI, Ying GS, et al. In vivo human choroidal thickness measurements: evidence for diurnal fluctuations. *Invest Ophthalmol Vis Sci*. 2009;50:5–12.
26. Tan CS, Ouyang Y, Ruiz H, Sadda SR. Diurnal variation of choroidal thickness in normal, healthy subjects measured by spectral domain optical coherence tomography. *Invest Ophthalmol Vis Sci*. 2012;53:261–266.
27. Agawa T, Miura M, Ikuno Y, et al. Choroidal thickness measurement in healthy Japanese subjects by three-dimensional high-penetration optical coherence tomography. *Graefes Arch Clin Exp Ophthalmol*. 2011;249:1485–1492.
28. Bland JM, Altman DG. Statistical methods for assessing agreement between two methods of clinical measurement. *Lancet*. 1986;1:307–310.
29. Katome T, Mitamura Y, Nagasawa T, Eguchi H, Naito T. Quantitative analysis of cystoid macular edema using scanning laser ophthalmoscope in modified dark-field imaging. *Retina*. 2012;32:1892–1899.
30. Twelker JD, Mitchell GL, Messer DH, et al. Children's ocular components and age, gender, and ethnicity. *Optom Vis Sci*. 2009;86:918–935.
31. Moreno TA, O'Connell RV, Chiu SJ, et al. Choroid development and feasibility of choroidal imaging in the preterm and term infants utilizing SD-OCT. *Invest Ophthalmol Vis Sci*. 2013;54:4140–4147.
32. Selovic A, Juresa V, Ivankovic D, Malcic D, Selovic Bobonj G. Relationship between axial length of the emmetropic eye and the age, body height, and body weight of schoolchildren. *Am J Hum Biol*. 2005;17:173–177.

Investigative Ophthalmology & Visual Science